CERN-PPE-94-113

EUROPEAN ORGANISATION FOR NUCLEAR RESEARCH

CERN PPE/94-113

July 7, 1994

First Measurements with a Diamond Microstrip Detector

F.Borchelt[8],W.Dulinski[3],K.K.Gan[5],S.Han[4],J.Hassard[2],A.Howard[2], H.Kagan[5],D.R.Kania[4],R.Kass[5],G.Lu[8],E.Nygard[6],L.S.Pan[4], S.Schnetzer[7],R.Stone[7],J.Straver[1],R.J.Tesarek[7],W.Trischuk[1], P.Weilhammer[1],C.White[5],R.L.Woodin[8],S.Zhao[5].

Abstract

We have constructed the first high resolution strip detector using chemical vapor deposited diamond as the detection medium. Devices produced with this material have the possibility of being extremely radiation hard with direct applications at high luminosity colliders. This paper details the detector material, the low noise readout electronics and the detector module. First results from a test with high momentum charged particles in a testbeam at CERN are described. We achieved a signal-to-noise of 6 : 1 and an efficiency of 85% for minimum ionizing particles in the testbeam. The detector has a strip pitch of 100μm and a strip width of 50μm. The measured position resolution we achieved was $\sigma = 26\mu$m. Future development of diamond detectors with application in particle physics experiments and other fields is discussed.

1 CERN, CH-1211, Geneva 23, Switzerland
2 Imperial College, Prince Consort Rd., London SW7 2AZ, United Kingdom
3 LEPSI, CRN Strasbourg 67037, France
4 Livermore National Laboratory, Livermore, CA 94551, U.S.A.
5 The Ohio State University, Columbus, OH 43210, U.S.A.
6 University of Oslo, 0316 Oslo 3, Norway
7 Rutgers University, Piscataway, NJ 08855-0849, U.S.A.
8 St.Gobain/Norton Diamond Film, Goddard Rd., Northboro, MA 01532, U.S.A.

Submitted to Nuclear Instruments and Methods A.

1 Introduction

High precision silicon microstrip detectors have become an important tool to improve charged particle track reconstruction and to study long lived particle decay vertices in high energy physics experiments. While the continued use of silicon detectors in these applications is being studied [1] it is becoming apparent that silicon detectors will only survive the intense radiation environment in limited regions of the detectors currently being planned for the LHC and elsewhere. In order to perform experiments at future high energy and high luminosity hadron colliders it is essential to develop detector technologies which are capable of withstanding high rates and particularly severe environments.

Detectors based on diamond could have advantages over silicon because of their potential radiation hardness and fast charge collection [2]. The practical use of diamond as a detector material has been made possible by recent advances in the chemical vapor deposition (CVD) growth process. This process allows diamond to be produced economically over a large area and with high purity. The use of CVD diamond as a charge collection material has recently been demonstrated by measurements using diamond as the active material in a sampling calorimeter [3]. This work provided a first look at the charge collection properties of diamond in a high energy physics application where many charged particles are produced. Having demonstrated the sensitivity of diamond to ionizing particles, our interest turns to applications which use diamond as a single charged particle tracker. A vertex detector at the heart of a hadron collider experiment is an ideal application for diamond in high energy physics. This paper demonstrates that such an application is possible.

After a brief description of the properties of diamond we describe the processes that went into preparing the diamond samples used, the preparation of the strip electrodes on the surface of the diamond, the low noise VLSI electronics used to read out the strips and tests in the laboratory with sources used to calibrate the detector and the electronics. Finally, we describe the testbeam telescope used to collect the track data and present the first results of the detector's spatial resolution and efficiency.

2 Principles of Operation

Some of the material properties of diamond which make its use attractive in the hostile environment of future colliders are shown in table 1 [2]. For the purposes of constructing high precision, radiation hard microstrip detectors, the parameters of interest are the large band gap and low intrinsic carrier density which imply low leakage currents, the large resistivity that allows ohmic contacts to be used to sense the charge created during ionization, the large breakdown voltage that gives stable operation, and the large cohesive energy and tightly bound structure which imply good radiation resistance.

In fig. 1 we show a schematic view of a single-sided diamond strip detector. The basic detector consists of a diamond wafer approximately 300 μm thick, a series of strips on one side of the diamond and a solid electrode on the opposite side. One applies an electric field, less than the breakdown field, across the thickness of the diamond. Under these circumstances the leakage current due to intrinsic carriers is extremely small on the order of a few picoamps. A charged particle traversing the diamond creates electron-hole pairs which separate in the applied field. The motion of these charges induces a current in the electrodes on the surface of the material; the size of this signal is proportional to the distance the charges separate. The average distance the electron-hole pairs separate is called the collection distance [4]

Table 1: Physical properties of diamond

Property	Diamond
Band Gap [eV]	5.5
Breakdown field [V/cm]	10^7
Resistivity [Ω-cm]	$> 10^{11}$
Intrinsic Carrier Density [cm^{-3}]	$< 10^3$
Electron Mobility [$cm^2V^{-1}s^{-1}$]	1800
Hole Mobility [$cm^2V^{-1}s^{-1}$]	1200
Saturation Velocity [μm/ns]	220
Dielectric Constant	5.6
Cohesive Energy [eV/atom]	7.37
Energy to create e-h pair [eV]	13
Mass Density [gm/cm^3]	3.5
Ave Number of e-h Pairs Created/100 μm [e]	3,600

and is used as a measure of the quality of diamond. The collection distance of the diamond described in this paper was $\sim 50\mu$m.

Figure 2 shows the collection distance as a function of the bias voltage applied across the diamond characterised with a ^{90}Sr source and a solid electrode [5]. In the testbeam we operated the diamond at 150 and 195 V where the collection distances were 45 and 49 μm respectively. In order to interpret the source collection distance measurements two corrections are necessary. First, electrons from the ^{90}Sr source were required to be almost minimum ionizing by demanding that they pass through the diamond and trigger a scintillator behind the detector. The diamond signals were then averaged by a digital oscilloscope. The ^{90}Sr electrons actually produce 8% more charge than a minimum ionizing particle. Second, the quantity most often used to characterize the signal in a microstrip detector is the most probable charge deposited by a particle and not the average charge which was measured in this characterisation. This is an important difference as the most probable charge deposited, Q_{mp}, is 1.6 times less than the average. Thus we have

$$Q_{mp} = d \times \frac{3600e}{100\mu m} \times \frac{1}{1.08} \times \frac{1}{1.6}. \quad (1)$$

The largest uncertainty here comes from the energy required to create an electron-hole pair in diamond, which we take conservatively to be $\pm 10\%$. Thus we expect most probable signals of 940 ± 95 electrons at 150 V and 1020 ± 100 electrons at 195 V.

3 Diamond Preparation

The microstrip detector used in the tests was fabricated using diamond from a chemical vapor deposition process [6]. In the CVD process [7] diamond is grown from a hydrocarbon gas which is mixed with hydrogen and excited by a power source, for instance a DC arc-jet. CVD diamond typically grows in a polycrystalline columnar structure. The substrate side begins with small grains ($\sim 1\mu$m) which coalesce and increase in size with material thickness. As the material is deposited it develops the texture of the fastest growing crystal orientation. The CVD diamond used here had a random orientation on the substrate and a (110) texture

on the growth side. It has recently been shown [5, 8, 9] that the electrical properties of CVD diamond improve with the thickness of the material: the collection distance is nearly zero on the substrate side and largest on the growth side. The raw CVD diamond material used was grown 550 μm thick of which 225 μm was removed from the substrate side and 25 μm was removed from the growth side. The removal of material from the substrate side increased the collection distance by 40% over the as-produced sample. Material was removed from the growth side in order to obtain a flat surface.

Before contacts were applied, the diamond was cleaned using two procedures. The first procedure was used to remove graphite, grease and residue from the thinning process. In this procedure the diamond was cleaned using a saturated solution of chromic acid; rinsed with de-ionized water; cleaned in dilute solutions of ammonium hydroxide and hydrochloric acid and finally rinsed in deionized water. The second procedure was used to remove any traces of chemicals, fingerprints, etc. In this procedure the diamond was cleaned in ammonium hydroxide; rinsed with de-ionized water, acetone, methanol, and de-ionized water; and then placed in an oxygen plasma etcher for final surface preparation. This processing is greatly facilitated by the chemical inertness of the diamond material itself.

4 Detector Design and Construction

The microstrip detector was constructed with 100 μm pitch and 50 μm strip width (see fig. 1). Initial source tests showed that with a strip pattern covering 50% of the active area there was no loss of charge relative to 100% coverage. The overall design of the detector is shown in fig. 3. The detector was constructed on an 8 mm $\times$ 8 mm $\times$ 300 μm diamond. The 64 strips were 6.4 mm long. A guard ring was provided in case edge leakage currents became a problem and a shorting bar was used to gang strips into a single readout channel for initial testing.

A metallic thermal evaporation technique was used to coat both sides of the diamond with successive metals: Cr (500 Å) and Au (3000 Å) [5]. This produced metal layers that were easily etched to make the readout strip pattern. Chromium was used since it easily forms a carbide structure; Au was used to prevent oxidation of the Cr layer and for ease of wire bonding. The evaporations were performed successively, first Cr from a Cr coated tungsten wire and then the gold from an alumina coated tungsten evaporation source boat. A shield between the two metal sources prevented contamination of the Au with Cr and vice-versa. The thickness of the metallic layers was measured during evaporation with an in-situ thickness monitor.

After metallizing each side of the diamond, the strip pattern shown in fig. 3 was created using a wet etch process. The sample was mounted on a silicon carrier wafer for ease of handling and to protect the solid metal side during the etching of the pattern side. Photo-resist was applied to one surface and baked at 90°C. The photo-resist was exposed using a mask of the pattern in fig. 3. The patterned sample was baked at 120°C for approximately 30 minutes. The unwanted metal was etched away and the photo resist removed with acetone. The sample was rinsed with deionized water and annealed at 580°C in an N_2 environment to allow the chromium to form a carbide with the diamond.

Generally, the metal in contact with the diamond determines the electrical properties of the contact. Chromium, titanium and other transition metals that form carbides tend to produce ohmic contacts to diamond. A current-voltage curve from a gang of six strips is shown in fig. 4 indicating high resistivity and low leakage currents (inset). At approximately

100 V the slope of the IV curve changes due to a saturation of the carrier mobility, an increase in the number of carriers and a change in the resistivity of the material.

In fig. 5 we show a block diagram of how the detector was connected to the external electronics. The circuit shown in fig. 5 was made on a 1 mm thick G10 printed circuit board which had a 7×7 mm^2 hole under the active region of the diamond to minimize the material in the path of particles traversing the detector. The detector was glued around the edges of this hole with a silver loaded conductive glue, DOTITE [10], to provide an electrical connection for the detector biasing voltage. In this design, each strip was DC-coupled (wire-bonded) to an individual preamplifier channel. The detector bias voltage was filtered locally and applied to the common electrode. A test input was provided with a 5:1 divider to facilitate the pulsing of the entire device from the common electrode. In addition, a standard 1.8 pF capacitor was bonded to a preamplifier channel in order to test and calibrate the electronics.

As with other microstrip detectors, the noise associated with the detectors should be small compared to that produced in the electronics. The noise contribution from the detector originates from four sources [11] (1) shot noise due to the statistical fluctuations in the leakage current; (2) bias resistor noise, (3) trace resistance noise and (4) detector load capacitance. In diamond the first term is expected to be small since the leakage current is small. In our detector the leakage current was measured at the operating voltage to be less than 1 nA for the whole detector. For a typical signal shaping time of 2 μs, a 1 nA leakage current produces $\sim$ 150 electrons noise. Assuming that this is shared uniformly among the 64 strips single channel noise should be less than 20 electrons. The small leakage currents allowed the diamond detector to be DC-coupled to the preamplifiers. In this case the bias resistor was effectively the feedback resistor of the preamplifier. This feedback resistor was more than 100 MΩ and hence it contributed less than 70 electrons to the noise. The third source of noise depends on the strip resistance. In our detector the strip resistance was measured to be $\sim$ 15 Ω which is about $\frac{1}{15}$ of the equivalent channel resistance of the input FET in the preamplifier. Again this noise contribution can be neglected. Finally, the load capacitance is less than 0.1 pF, and thus also contributes a negligible amount to the overall noise (discussed in the next section).

5 The Low Noise VIKING Preamplifier

The detector was connected to VIKING readout electronics [12] through 25μm diameter aluminium wire bonds which were wedge bonded to the gold readout electrodes and preamplifier inputs. The VIKING is a 128 channel VLSI CMOS chip. Each channel contains a charge amplifier, followed by a CR-RC shaper with a 2μs peaking time[1] and a sample-and-hold circuit. The charge from each channel is output sequentially using a multiplexer and shift register which are integrated in the chip. The noise performance of the VIKING has been measured to be [13]:

$$ENC = 135 + 13 * C_{tot} \quad electrons \tag{2}$$

where C_{tot} is the total detector capacitance seen at the input of the amplifier. It has been shown [11] that the $\frac{1}{f}$ noise and the FET bulk resistance noise do not contribute significantly and that the main effect comes from the channel noise. With a measured strip capacitance of

[1]This peaking time is variable, but with the inherently low leakage currents in the diamond it was optimal to make this time as long as possible for best noise performance.

less than 1 pF the expected total noise is less than 150 electrons, neglecting all other sources of noise from the detector.

The G10 board carrying the detector and its biasing electronics was glued next to the readout chip and the readout electrodes were wire-bonded to individual VIKING preamplifier channels. A photo of the final assembly is shown in fig. 6. The readout chip was supported on a ceramic substrate with simple routing lines which provided the 24 control signals necessary for the VIKING operation. A repeater card placed 10 cm away from the ceramic substrate received and regenerated the timing signals and ran a line driver capable of transmitting the analog output of the VIKING a distance of 30 m to the counting room. This repeater card also generated the analog voltages necessary for VIKING operation. For the first time in a beamtest the VIKING was operated with a set of linear power supplies allowing the chip noise performance to approach that seen in laboratory tests (eqn. 2).

6 Calibration of Preamplifier Noise Level

Two calibrations of the readout electronics were performed. The first used the 1.8 pF capacitor which allowed a known equivalent charge signal to be fed into the front end of a single preamplifier. In the laboratory we measured a typical single channel noise of 4 counts. With a 0.68 ± 0.05 mV pulse fed into the 1.8 pF capacitor (a 7600 electron equivalent signal) we digitised this signal at 240 ± 4 counts and hence concluded that the single channel noise was 128 electrons. The principle uncertainty on this calibration comes from potential stray capacitance at the input of the amplifier which may add to the 1.8 pF external capacitor and thus increase the equivalent signal seen. Typically such stray capacitance is less than 0.5 pF while the nominal capacitance is good to $\pm 10\%$. Thus we conclude that the noise is:

$$ENC = 128^{+31}_{-13} \quad electrons. \tag{3}$$

In the second calibration procedure a 2×2 mm^2 DC-coupled silicon diode was bonded to another preamplifier. We measured the 59 KeV photon signal produced by ^{241}Am in this silicon diode. This provided a signal of $59000/3.6 = 16400$ electrons. The photons used in this measurement deposited all of their energy in the silicon; Compton scattered photons were rejected by setting the trigger threshold at 3/4 of the peak signal value. A digital oscilloscope averaged the signal from the silicon. The ^{241}Am photon produces a 580 ± 15 mV average signal. The capacitor calibration provided the cross-calibration (307 ± 10'mV for 240 ± 4 counts independent of any stray input capacitance) to interpret the ^{241}Am signal in counts. Thus 16400 electrons corresponded to 453 ± 20 counts. Here the precision was limited principally by the accuracy of the oscilloscope which we used to make the measurements. From this calibration the noise is determined to be:

$$ENC = \frac{16400(electrons)}{453 \pm 20(counts)} \times 4(counts) = 144 \pm 6 \quad electrons. \tag{4}$$

These two calibrations were performed on preamplifier channels which were not bonded to the diamond readout electrodes themselves. The backplane pulsing circuit and the expected uniform capacitive coupling of the readout electrodes provide a cross check of the gain uniformity from channel-to-channel in the VIKING. A spread of 10% was observed in channel gain (assuming that all channels except those at the edge of the detector were coupled capacitively to the backplane in the same way). Taking the channel-to-channel gain variation

as a conservative estimate of the possible uncertainty and averaging the two previous noise calibrations we arrive at a final estimate of the single channel noise of:

$$ENC = 140 \pm 15 \quad electrons. \tag{5}$$

in good agreement with the expectations in section 5.

7 Testbeam Setup

The spatial resolution measurement of the diamond detector was measured in a 50 GeV pion testbeam at CERN, using a telescope of eight silicon microstrip reference detectors. The reference detectors were single–sided, AC–coupled, 3×6 cm^2 silicon detectors with an implant/readout pitch of 25/50 μm, equipped with MX3 [14] electronics. They were arranged in 4 X–Y pairs where each pair was connected to one readout processor (SIROCCO) as shown in fig. 7. The individual reference detectors had a resolution, σ, of 6.5 μm, which resulted in an interpolation error of 3.5 μm in the plane of the diamond. This was more than adequate for the resolution we expected to achieve with this first diamond detector. All detectors were mechanically mounted on a granite/steel optical bench with an intrinsic precision of better than 1 mm. A trigger was provided by a pair of 1×1 cm^2 scintillators.

The VME/OS9 based DAQ system [15] provided the clock signals for both the microplex chips of the reference detectors and the VIKING readout chip of the diamond detector. Using a coincidence of the microplex livetime and the scintillator trigger, the VIKING chips were triggered and the event was read into the VME–SIROCCO buffers. The system was controlled by a VME Eurocom 6 processor. All raw data were written to EXABYTE tape for later analysis. A subset of the data was analyzed online, to provide monitoring.

8 Results

The results presented in this section are based on two analyses. Both use a common procedure for extracting the silicon signals from the raw data. The first analysis is based on a cluster hit search algorithm in the diamond and attempts to match hits found with tracks in the silicon. The second uses the silicon information to measure the charge seen in the diamond in a way which is unbiased by the diamond information itself.

Data were taken with normally incident beam particles. The results presented here were measured at diamond bias voltages of 150 V and 195 V. We concentrate on the 150 V data sample as it contains twice as many tracks and is better understood than the 195 V sample. We describe the processing used to extract hits from the raw data for the silicon telescope counters and the diamond detector. Next the results of a clustered hit search on the diamond are described and finally the results of an unbiased search for signals on the diamond using tracks extrapolated from the silicon. These studies indicate that all the charge expected from the diamond was collected in our measurements and the position resolution of the diamond is consistent with the signal-to-noise performance achieved.

Raw Data Processing

Since the raw data for all detector strips from every event are written on tape, the pedestals, single channel noise, N (computed as the root mean square fluctuations about

the channel pedestal), digital common mode noise corrections and finally the signal pulse heights were computed offline. The noise and pedestal were continuously updated using a digital filtering algorithm [15], which avoids including actual charged particle hits in the computations. Possible common mode baseline shifts were also computed and corrected on an event-by-event basis, but with the linear power supplies used these corrections were small, improving the single channel noise by only 10 – 20%. The noise and pulse height levels for all strips of the diamond detector were written to a summary file for later analysis.

For the silicon reference counters, a charge-cluster search for hits from beam particles was performed. Since the cluster parameters were not so well known for diamond, a similar search was performed after a scan of the parameter space. The cluster search method had three steps. First, all channels were scanned to find strips (seeds) with a signal higher than $4 \times N$, where N is the single strip noise level calculated above. Second, if such a seed strip was found then all neighboring strips with a signal above $2 \times N$ were added to form a cluster. Finally, the sum of the charge in all strips attached to a cluster in this way was finally required to be above $6 \times < N >$ (where $< N >$ is the single strip noise averaged over all strips included in the cluster). This procedure was continued until all seeds were exhausted. Seeds too close to the edge of the detector (within 5 strips) were not included in the cluster search, however this had no effect on the final analysis since the active area of the diamond was more than 1 cm from all edges of the telescope counters. The information for clusters found was then written into another summary file for later analysis.

The search for charge-clusters in the diamond detector was done as part of the final alignment procedure, using the same method as described above for the telescope reference detectors. In this way it was possible to easily alter the parameters in the cluster search streamlining our analysis.

Once the clusters were defined the particle hit positions were calculated using a non-linear interpolation algorithm. This algorithm was used for charge-cluster widths ≥ 2. Single strip clusters in silicon are less than 0.1% of all events. In this algorithm it was assumed that the beam illumination was uniform between all pairs of strips, and that the charge was collected by only two strips. For clusters with more than two strips the two adjacent strips with the highest sum pulse height were used. A quantity η is defined as follows:

$$\eta \equiv \frac{PH_r}{PH_l + PH_r} \tag{6}$$

Where $PH_{l,r}$ is the signal pulse height of the left,right strip in a cluster. The average impact position x for a given η value was obtained in the following way:

$$x = P_s \int_0^{\eta} \frac{dN}{d\eta'}(\eta')_n d\eta' + X_0 \tag{7}$$

Where P_s is the strip pitch, $dN/d\eta'(\eta')_n$ is the normalized $dN/d\eta'(\eta')$ distribution [2], and X_0 is the absolute position of the left strip in the cluster.

After defining the hit positions an iterative procedure was used to align the detectors. The first step used the telescope reference counters and tracks with hits in all x and y detectors. The outer detectors for the x and y coordinates were taken as a reference. Then the two inner x and y detectors were shifted and rotated iteratively until the residuals of the impact

[2]The $dN/d\eta'$ distribution is determined from the data itself (the number of particles per η') and the unfolding works because the beam illumination is uniform between all pairs of neighboring strips.

positions were minimal. The second step repeated this process for the diamond detector using the diamond hits in each event with the highest signal-to-noise ratio. After this step the optimal position of the diamond along the beam line (z coordinate) was determined by searching for the minimum variance of the residual distribution as function of z. In both steps χ^2 cuts were applied on the line fits and a $4 \times \sigma$ cut was placed on the reference detector residual distributions except for the final distribution of diamond hits.

Clustered Diamond Signal Results

Figure 8 shows a typical plot of the Landau shaped signal pulse height of cluster's charge and the distribution of the single channel noises for all strips, measured at $V_{bias} = 150$ V. This plot shows that the signal peak and the average measured noise level were separated by a factor of 6. The cluster-charge in this plot was obtained with the following parameters of the cluster search: $Q_{seed} = 2 \times N$, $Q_{neighbor} = 1 \times N$ and $Q_{total} = 2.5 \times < N >$. A scan over these parameters has been performed on each data sample using the following parameter relations: neighbor-cut = $0.5\times$ seed-cut and Q_{total}-cut = $0.5 \times N$ + seed-cut, with a step size of $0.25 \times N$. This scan showed that a seed-cut of $2.0 \times N$ gave the best performance for data samples taken at both bias voltages. The performance criteria were defined as an optimum between hit efficiency and a minimum of excess (noise) clusters. Reducing the cut levels increased the chance that noise was identified as a track hit while increasing the cut levels biased the cluster-charge measurement because clusters with little charge were removed.

The efficiency of the diamond was determined by comparing the number of tracks in the telescope and the number of clusters found in the diamond inside a window of 6×2 mm^2 on the active surface of the diamond detector as a function of the cluster search parameters. It showed only small variations around the parameters used for the results shown here. The efficiency for the data sample with $V_{bias} = 150$ V, was $82 \pm 3\%$ for hits within 100 μm of the predicted track position. For the data sample measured at $V_{bias} = 195$ V the efficiency was $86 \pm 4\%$.

The average number of clusters per event found with these cuts was 1.4. The beam intensity was sufficiently low to ensure that there was only one particle present in the telescope in any trigger. The extra clusters in the diamond are expected due to the very low cluster definition cuts, but the chance that such a cluster would overlap at random with a charged particle track was small ($\approx 60\%/20$(strips) $= 3\%$).

Figure 9 shows the S/N distribution measured at $V_{bias} = 150$ V for the clusters which were within 100μm of the reconstructed tracks in the telescope. The data are fit with an approximation to a Landau distribution [16], and the most probable value found in this way is S/N $= 5.78 \pm 0.13$. Also shown in fig. 9 is the relationship between the mean and most probable values of this Landau distribution. The ratio of these two numbers is 1.6 ± 0.1 for our dataset. For $V_{bias} = 195$ V the most probable value is 6.25 ± 0.18. Including a systematic uncertainty of ± 0.50 (units of S/N) and using the noise determined earlier, the S/N at $V_{bias} = 150$ V is equivalent to a most probable charge for a minimum ionizing particle of 810 ± 110 electron-hole pairs while at $V_{bias} = 195$ V it is 875 ± 115 electron-hole pairs. This is in good agreement with the charge expected from the diamond. The charge collected with a solid electrode (the characterisation described in section 2) is in good agreement with the charge collected on the strips, within the 15% uncertainties of this comparison.

The residual plot in fig. 10 shows the spatial resolution of the diamond detector measured at $V_{bias} = 150$ V. The distribution is fit with a Gaussian which has a sigma of 26.8 ± 0.6 μm.

Correcting for the telescope's interpolation uncertainty yields a resolution of 26.6μm. For the data sample measured at 195 V the corrected spatial resolution is 25.4 ± 0.9 μm. With the signal-to-noise attained these results show a 12% improvement with respect to the digital resolution which is $100/\sqrt{12} = 28.9$ μm. This improvement is in agreement with the expected scaling of hit precision with signal-to-noise.

The cluster width distribution for charge-clusters which lie on the reconstructed tracks is shown in fig. 11. This plot shows that while the majority of the clusters were only one or two strips wide there are a non-negligible number of clusters with significant charge on more than two strips. This is due to the charge collection mechanism in the diamond.

Transparent Analysis Results

Once the diamond detector was aligned in the reference frame of the beam telescope it was possible to search for charge deposited around the position where a particle passed through the diamond. This provided an unbiased measurement of the charge collection on the strips, and a cross check of the cluster search efficiency without biasing the signal seen on the diamond strips.

The signal (scaled to the single strip noise, N) found on the strips nearest the track extrapolation, for the data sample with $V_{bias} = 150$ V is shown in fig. 12. The five plots show the summed charge measured on 1, 2, 3, 4 and 5 strips respectively, chosen such that the sum of the distances, to the number of strips being considered, from the track position was minimal. Figure 13 shows the same five plots of measured charge but now for strips centered a distance of 1 mm from the predicted track position on the diamond. Comparing these two figures clearly shows that the signal deposited in diamond is well separated from the background noise levels.

The curves fit in fig. 12 are the sum of a Landau distribution plus a half-Gaussian noise contribution whose normalisation was determined as part of the fit, but whose width was constrained by the measurements of fig. 13. The most probable charge deposition for each number of strips is plotted in fig. 14 showing that charge was shared on two or three strips at most in our tests. The dashed curve in fig. 14 is the result of an electrostatic calculation of the image charges induced on the detector electrodes. Although the charge generated along the track path is uniform the separation of this charge and hence the signal induced varies linearly from one side of the diamond to the other. We modelled this as a linearly increasing signal density through the thickness of the diamond and integrated the charge induced on each strip as function of its distance from the position that the track passed through the detector. More details on this calculation (in particular for the case where material has been removed from the substrate side to improve the collection distance) can be found in reference [5].

9 Conclusions and Prospects

The results presented here indicate the feasibility of using diamond as the detection medium in a microstrip tracker. Achieving a signal-to-noise ratio of 6 : 1 and a position resolution of 26 μm allows us to consider diamond a viable alternative to silicon for future high energy physics experiments.

We expect to improve the diamond material itself in order to maximize the signal produced by minimum ionizing charged particles. Work is underway to prepare diamonds which will

produce twice the signal of the diamond used here. However for operation at the LHC, preamplifier shaping times much shorter than those used here (50 ns compared to 2 μs) must be realized. This will result in at least a 6-fold increase in the noise level of the electronics. Hence continued improvement in the material to increase the signal, coupled with a lowering of the noise level of the readout electronics is necessary. To be a viable alternative for tracking one would hope to operate at a signal-to-noise ratio of 15:1 with fast electronics.

References

[1] A.Chilingarov and S.Roe, *Radiation Damage Projections for Silicon*, ATLAS INDENT-No. 31.

[2] M. Franklin *et al.*, Nucl. Instr. and Meth. **A315** (1992) 39.

[3] R.J.Tesarek *et al.*, accepted for publication in Nucl. Instr. and Meth.

[4] L.S. Pan *et al.*, J. Appl. Phys. **74** (1993) 1086.

[5] S. Zhao, Ph.D. Thesis, The Ohio State University (1994).

[6] The CVD diamond was provided by Norton Diamond Film, Goddard Road, Northboro, MA 01532.

[7] J. Angus and C. Hyman, Science **241** (1988) 913; and W. Yarbrough and R. Messier, Science **247** (1990) 688.

[8] M.A. Plano *et al.*, Appl. Phys. Lett. **64** (1994) 193.

[9] S. Zhao *et al.*, Mat. Res. Soc. Symp. **Vol 302** (1993) 257.

[10] DOTITE is a heat sensitive silver loaded conducting glue manufactured by Fujikura Kasei Co., Sakae-machi, Sano-city, Tochigi-ken, Japan. This glue has the property that after curing the items joined may be separated by the addition of heat.

[11] E. Nygard *et al.*, Nucl. Instr. and Meth. **A301** (1991) 506.

[12] P. Aspell *et al.*, Nucl. Instr. and Meth. **A315** (1992) 425.

[13] O. Toker *et al.*, Nucl. Instr. and Meth. **A340** (1994) 572.

[14] J. Stanton and N. Kurtz; RAL–89–028 Rutherford Appleton Laboratory.

[15] R. Turchetta, Ph.D. Thesis, N. 1019, Strasbourg, France (1991).

[16] The approximation to a Landau distribution used here is:

$$L = p_4 exp[\frac{-1}{2}(G + e^{-G})]$$

where $G = p_3\frac{(x-p_1)}{(p_1-p_2)}$. The most probable value of the distribution is given by p_1.

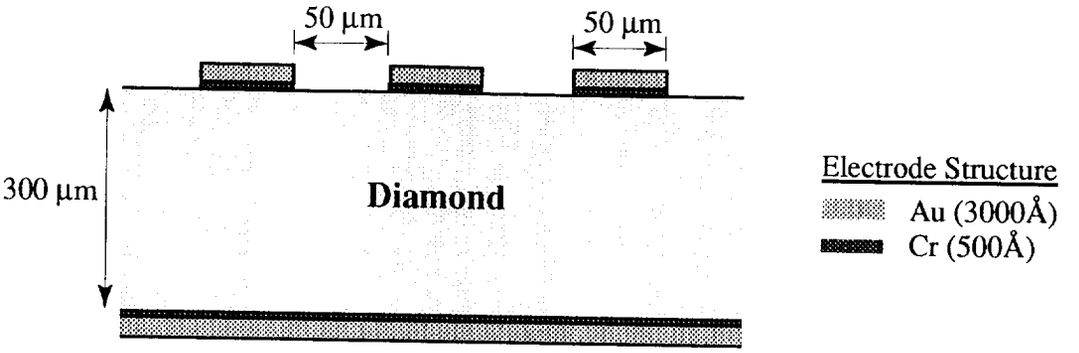

Figure 1: Cross section view of the diamond microstrip detector.

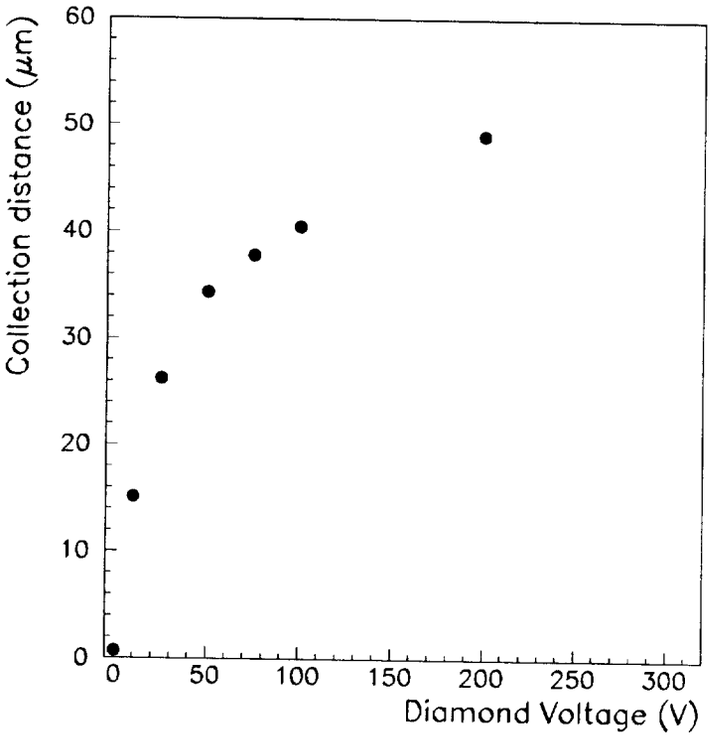

Figure 2: Charge collection distance as a function of bias voltage placed across the diamond. The uncertainty on the charge collected at each voltage is smaller than the size of the plotted points.

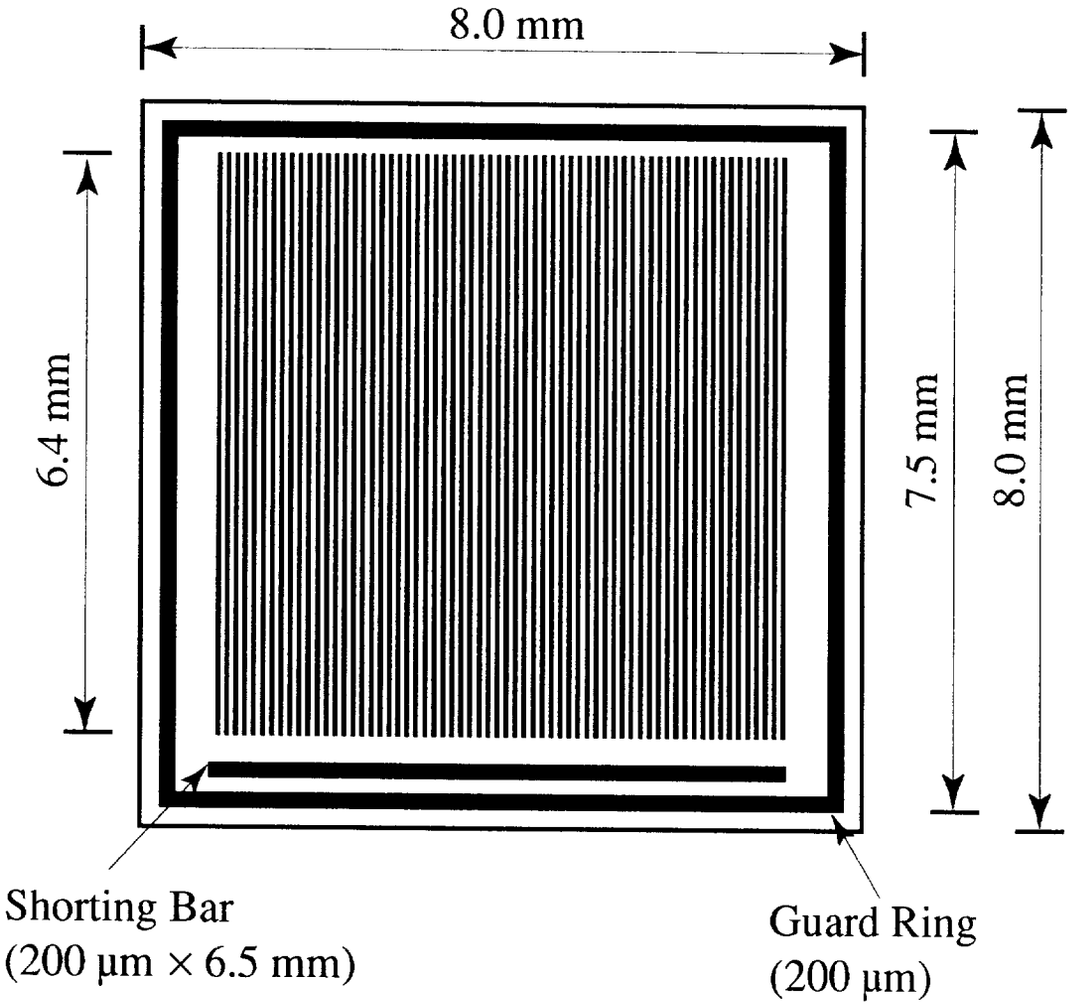

Figure 3: Schematic view of the diamond microstrip detector.

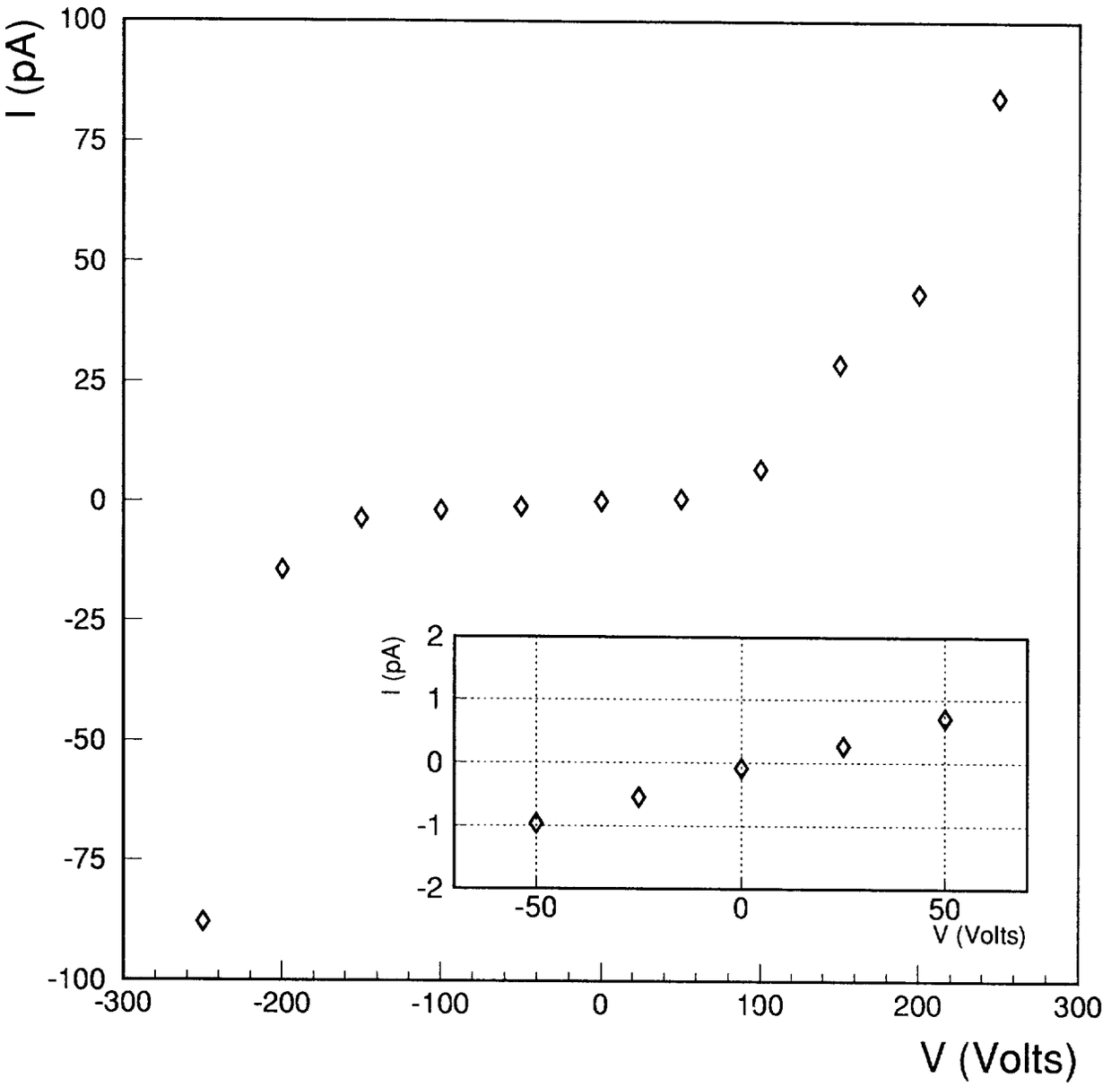

Figure 4: $I - V$ characteristics of six ganged strips from the diamond detector. The inset shows the resistive behaviour for bias voltages below 50 V.

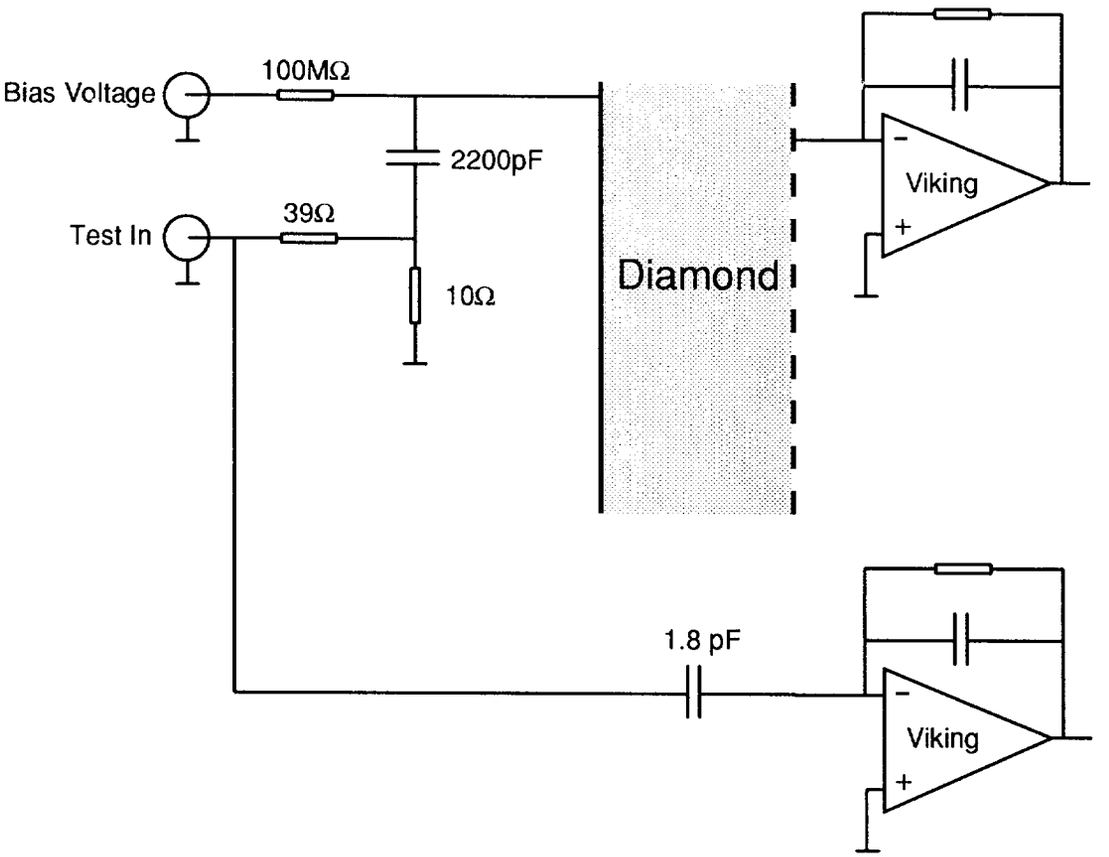

Figure 5: Block diagram of the support electronics for the diamond detector.

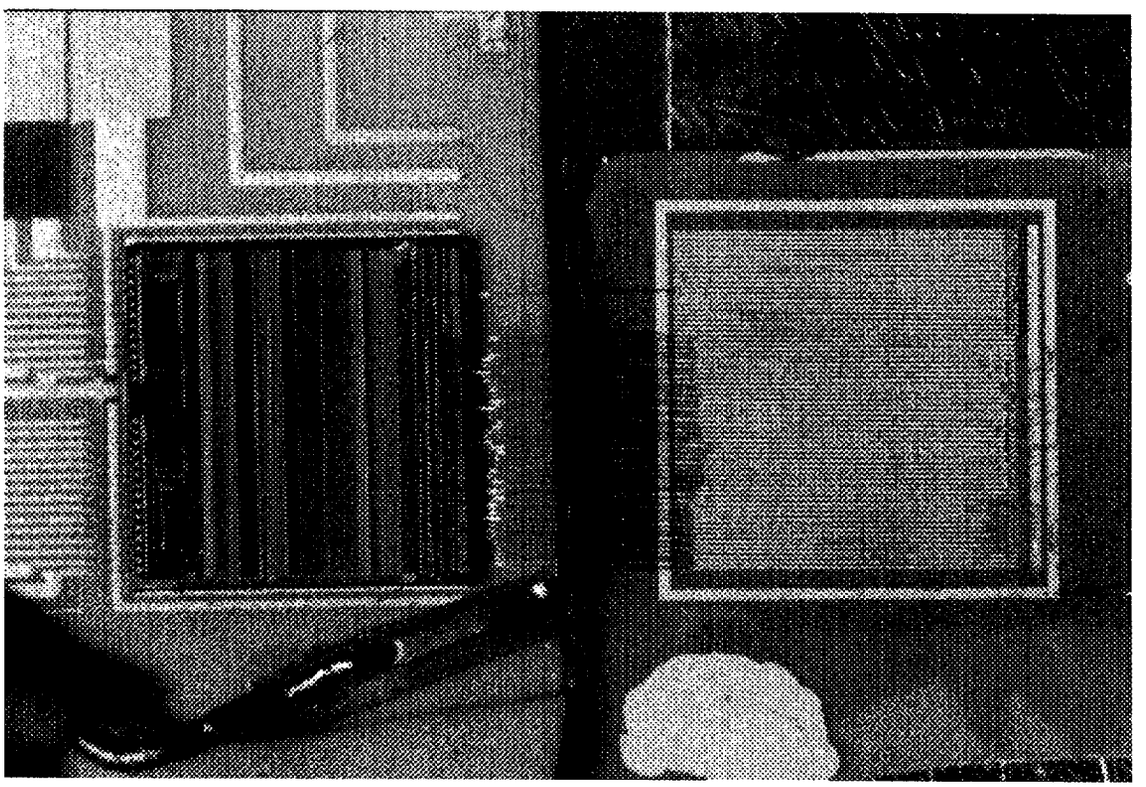

Figure 6: A photograph of the diamond detector and Viking readout chip.

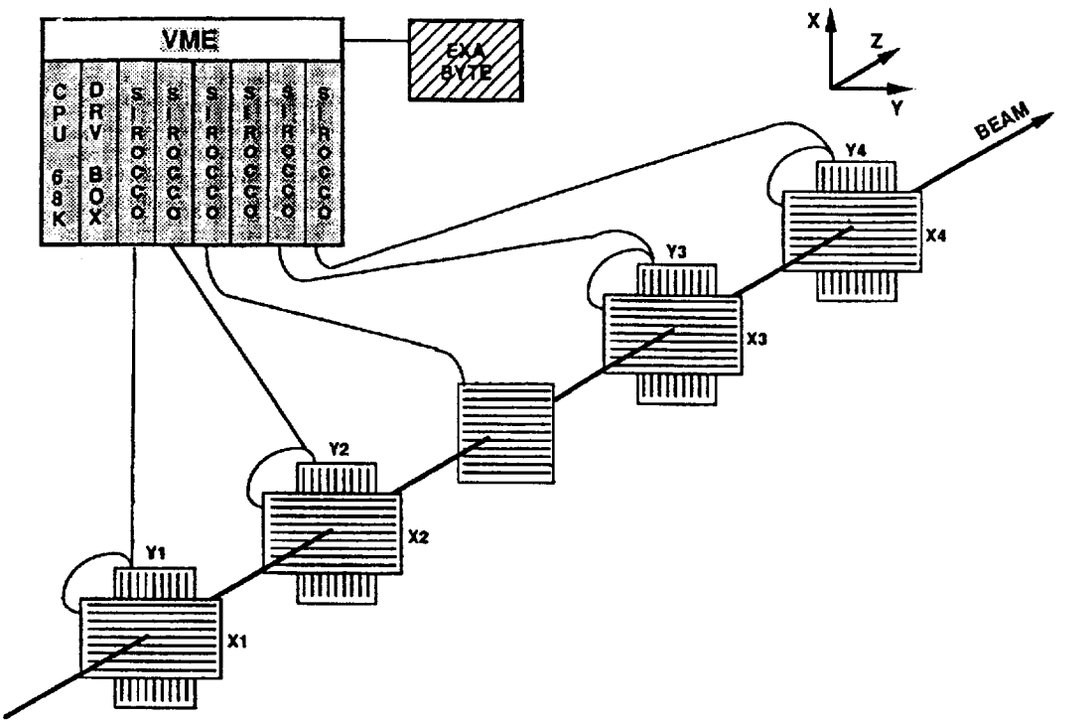

Figure 7: The beam telescope with 8 single–sided reference detectors (4 X and 4 Y) and the diamond detector.

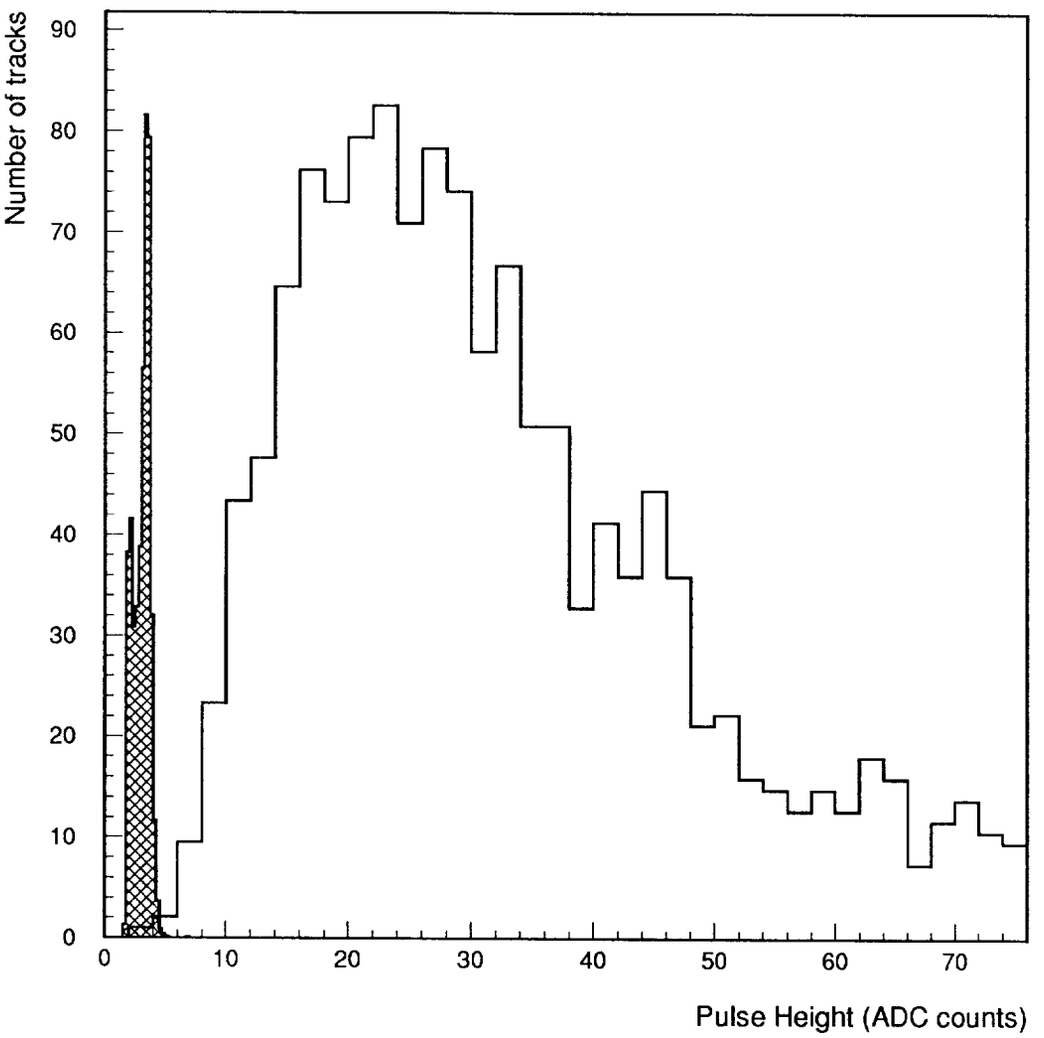

Figure 8: The pedestal-subtracted signal distribution with the pedestal width distribution (hatched) overlaid, with arbitrary normalisation, for comparison.

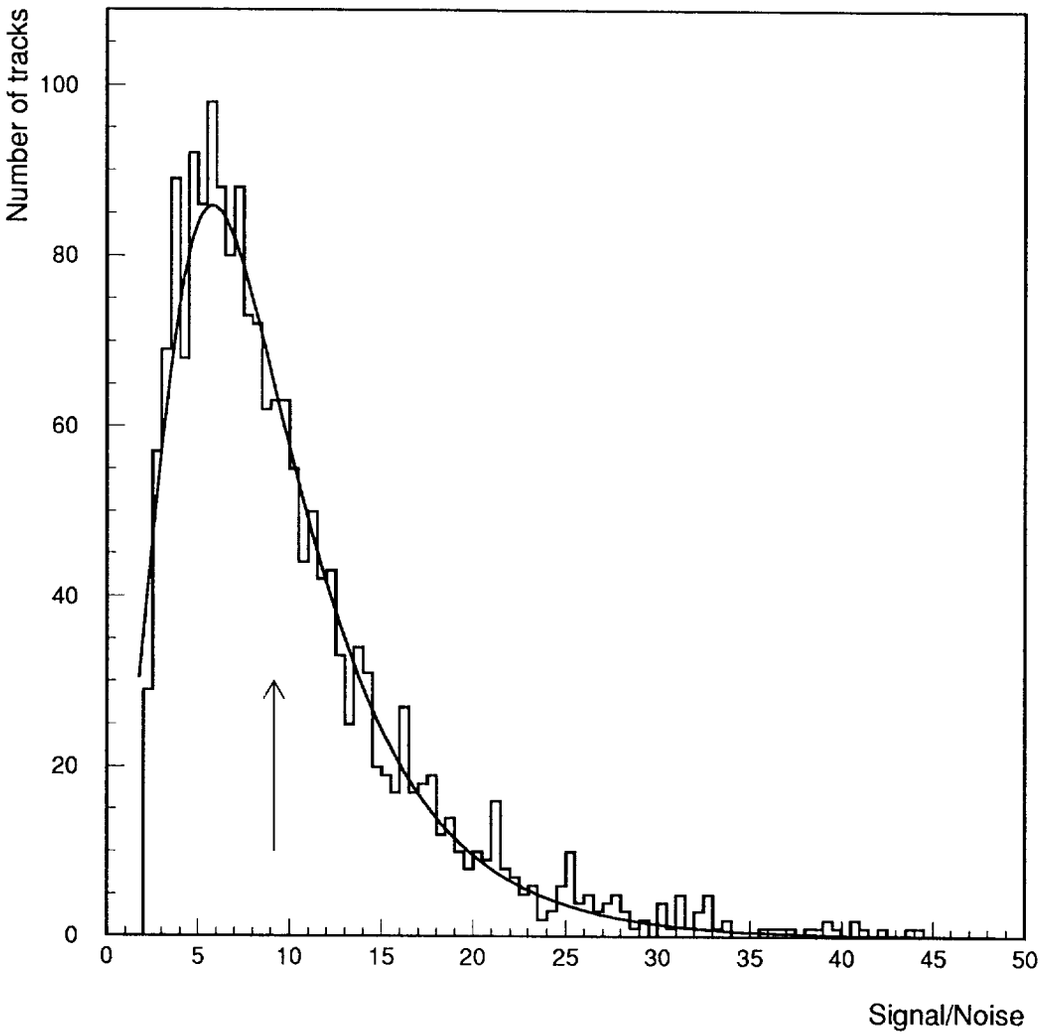

Figure 9: Signal-to-Noise distribution for hits which are well matched to charged particle tracks as predicted by the silicon telescope. The solid line represents a fit (described in the text) which gives a most probable signal is 5.78 ± 0.13 times the average single strip noise (N). The arrow indicates the average of this distribution which is 1.6 times higher than the most probable value for this S/N. These data were taken with a diamond bias voltage of 150 V. The most probable signal-to-noise was 6.25 ± 0.18 for a bias voltage of 195 V.

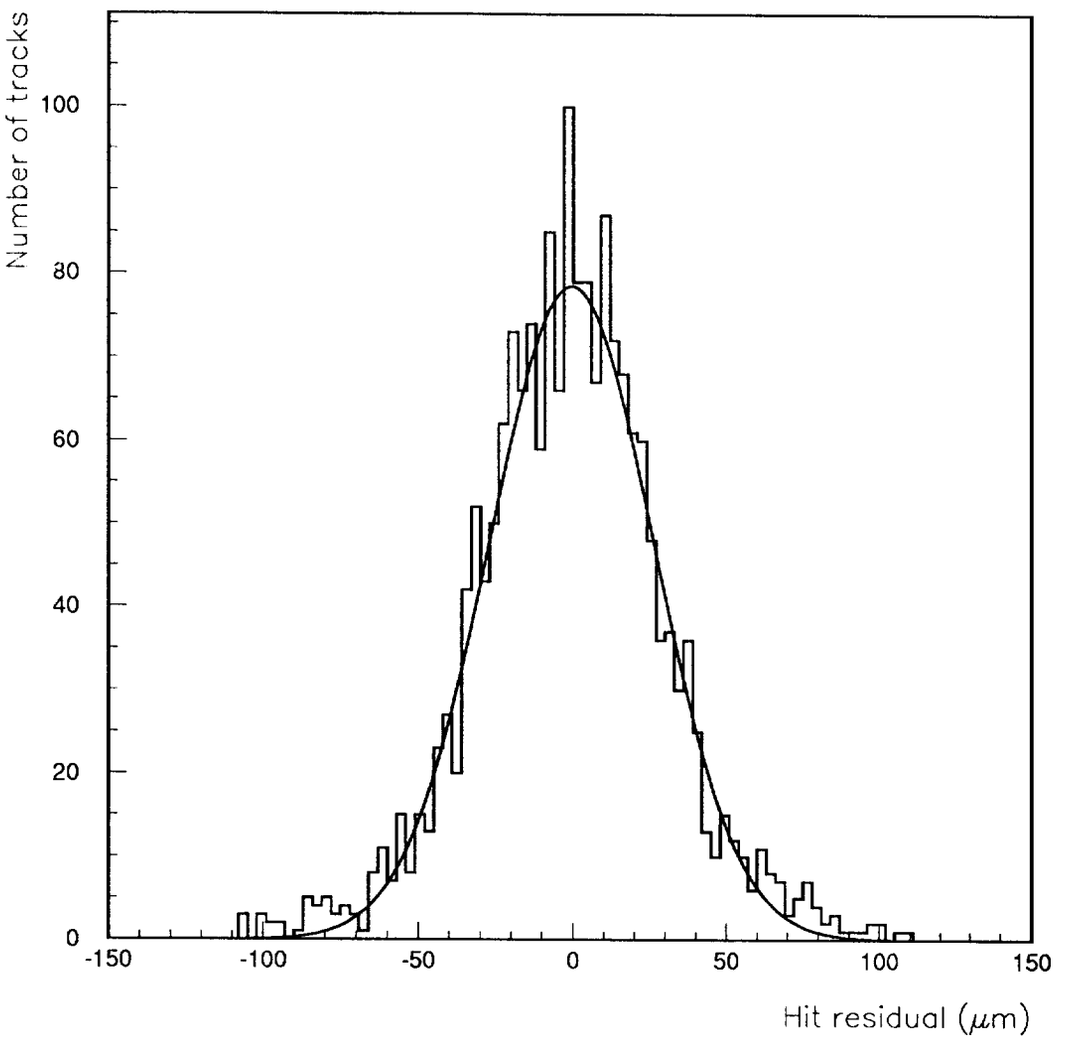

Figure 10: The experimental position resolution of the diamond detector, compared to the predicted charged particle impact point based on the silicon telescope information. The fit of a single Gaussian gives a sigma of 26 μm.

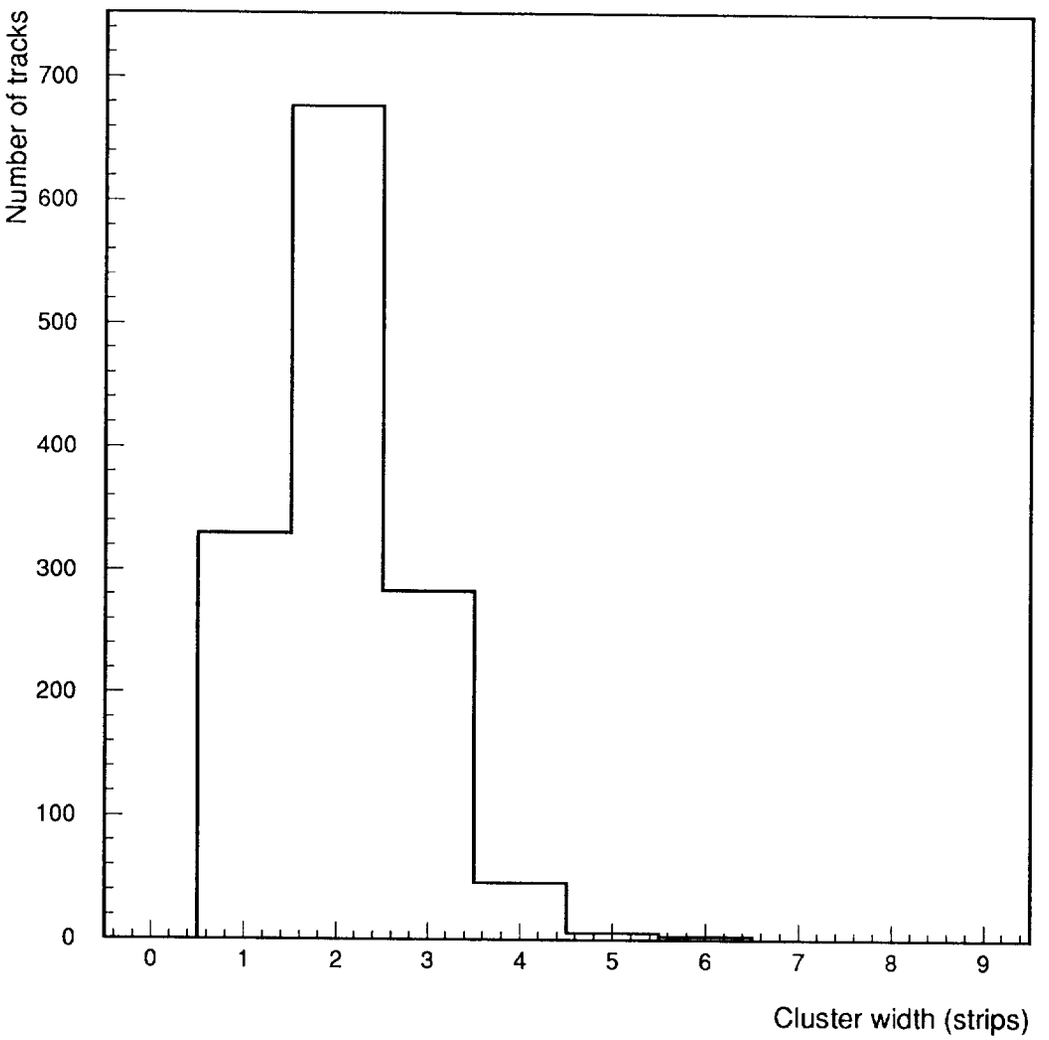

Figure 11: The number of strips which are included in diamond hit clusters.

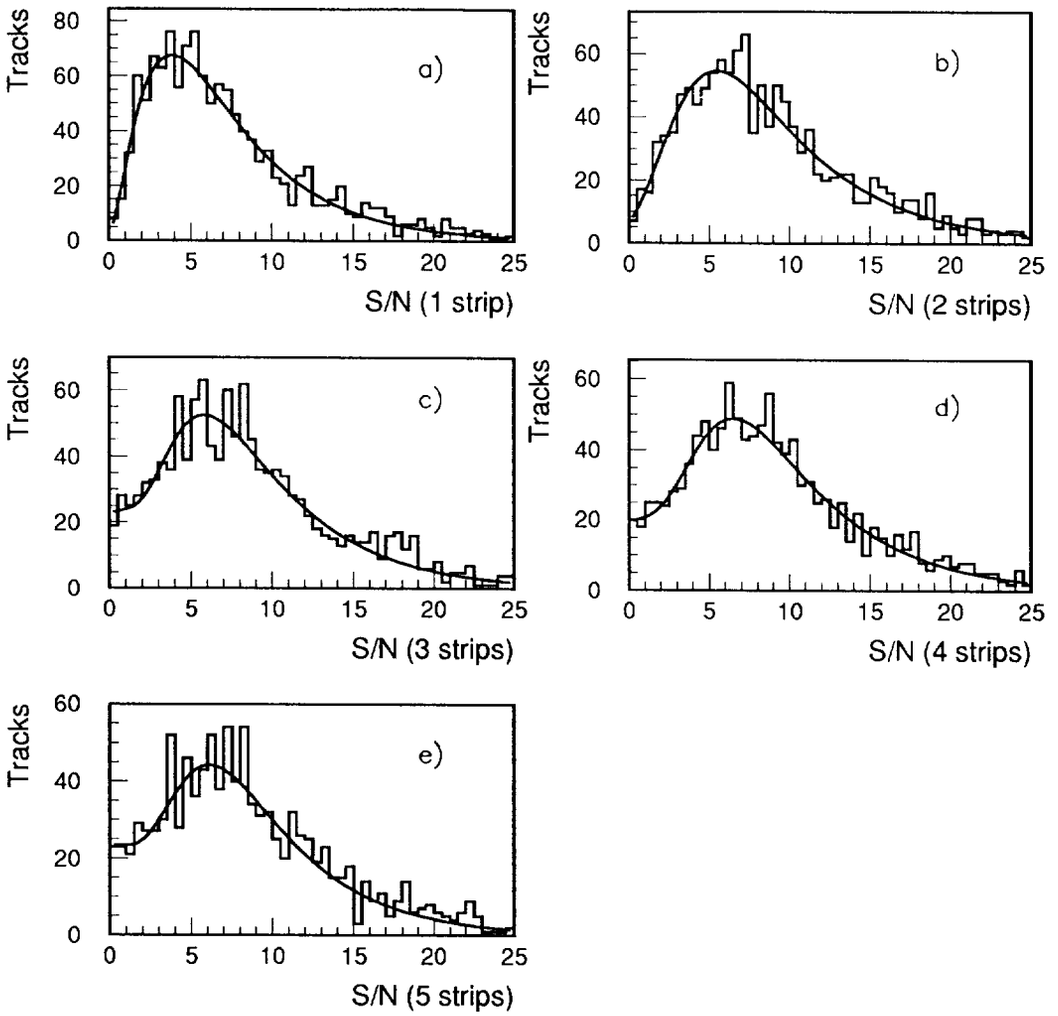

Figure 12: The signal-to-noise distribution on a) the strip nearest the track projected from the silicon telescope, b) the two strips nearest the projection, c) the three nearest strips d) the four nearest strips and e) the five nearest strips. The fits are a combination of a Landau distribution (for the signal) and a pedestal distribution (a Gaussian whose width was determined by the *off-track* hits in fig. 13). The most probable signal-to-noise values for these fits are plotted in fig. 14.

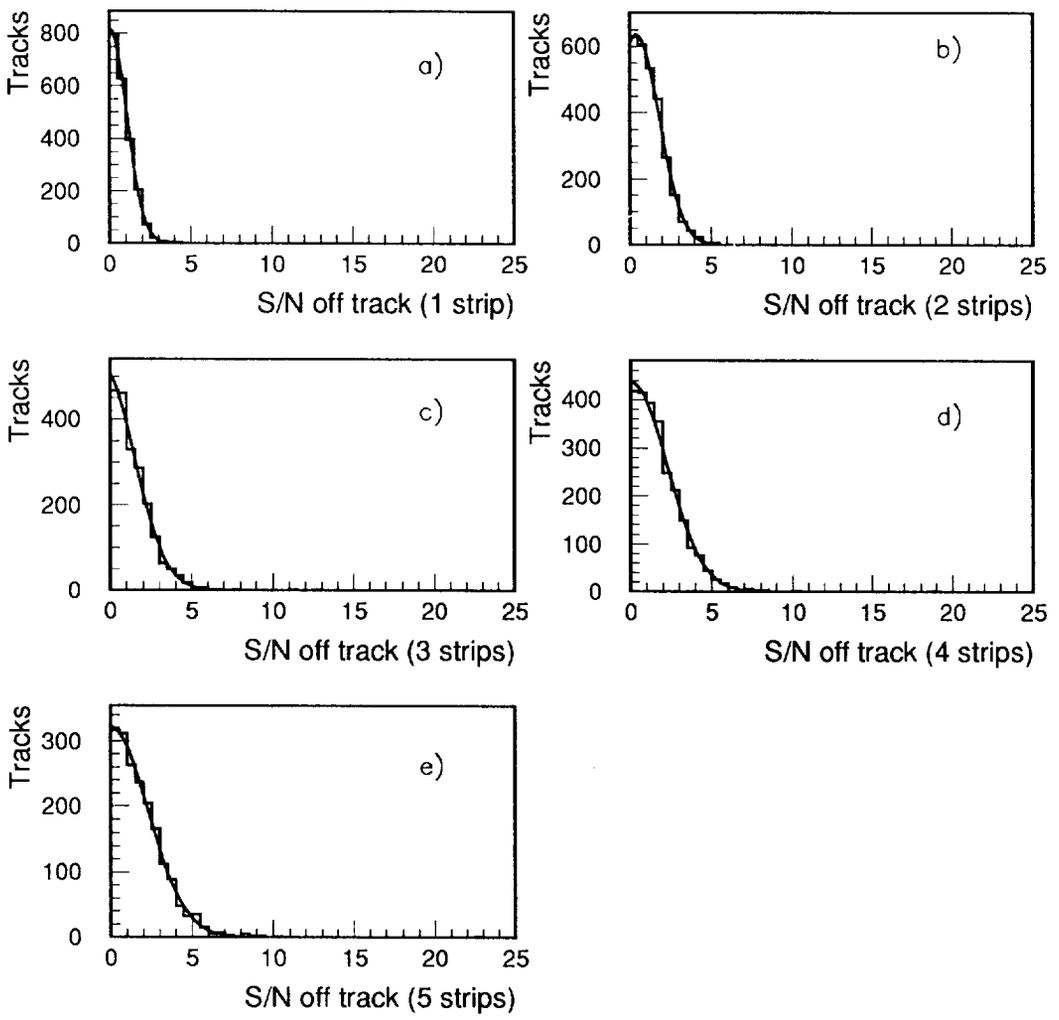

Figure 13: The signal-to-noise distribution on 1 to 5 (a) to e)) strips which are 1 mm away from the track projected into the diamond.

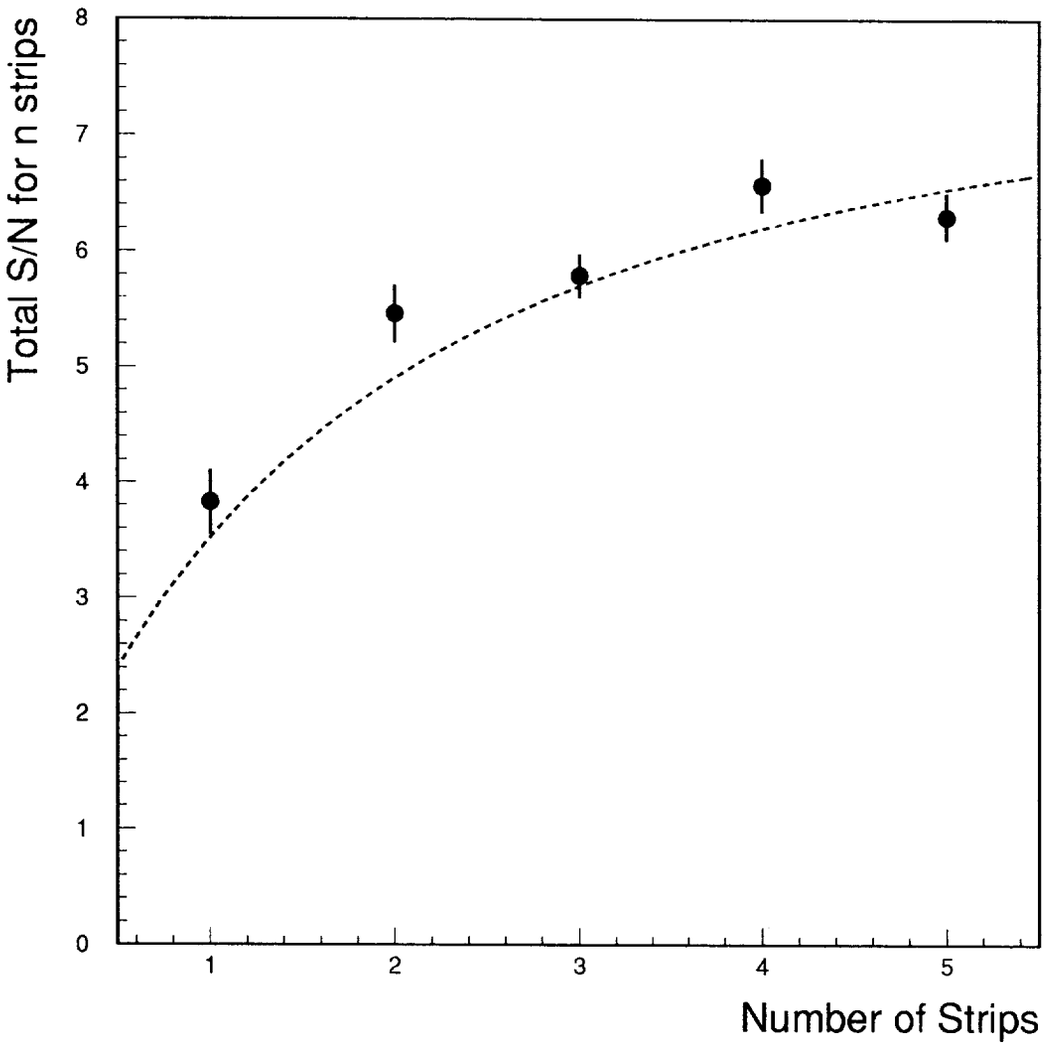

Figure 14: The most probable charge as a function of the number of strips included around the position of the projected track. The dashed line overlaid is the prediction of the simple electrostatic model, described in the text, for the charge sharing.